Vilnius University
Faculty of Physics

Gul Jan

# NOISE DIAGNOSTICS OF OPTOELECTRONIC DEVICES

Master's final thesis
Electronics and Telecommunication Technologies

| | |
|---|---|
| Student | GUL JAN |
| Approved | 2026-05-22 |
| Academic supervisor | doc. Sandra Pralgauskaitė |
| Director of the Institute | prof. doc. Robertas Grigalaitis |

Vilnius 2026

Table of Contents

## Introduction

Low-frequency noise (LFN) analysis is an important diagnostic method for investigating the quality, reliability, and degradation mechanisms of optoelectronic devices such as light-emitting diodes (LEDs) [1],[2],[3]. Compared to conventional electrical characterization techniques, noise measurements provide higher sensitivity to microscopic defects, carrier transport fluctuations, and structural imperfections that may not be detected through standard current–voltage or optical measurements [1],[4], [5].

InGaN semiconductor structures based blue light-emitting diodes are widely used in illumination systems, display technologies, optical communication and sensing applications due to their high efficiency, compact size and long operational lifetime [2], [6]. However, defects, leakage currents, thermal stress and aging processes can strongly affect the performance and reliability of LEDs, which can influence both the electrical and optical characteristics [6], [10]. The effects are observed as fluctuations of current, voltage and emitted light intensity, usually seen as low frequency noise [5].

The $1/f$ noise is of particular importance for different noise mechanisms, as it is closely related to carrier trapping, recombination processes and defect states within the semiconductor structure [5], [7]. Electrical noise is related to fluctuations in the carrier transport, and optical noise is related to fluctuations in the intensity of emitted light. The correlation between electrical and optical fluctuations is a useful indicator of the device operating conditions, degradation mechanisms and material quality [2], [6].

In this work, the low-frequency electrical and optical noise properties of two blue LEDs with peak wavelengths 455 nm and 470 nm are studied experimentally before and after accelerated aging. The dependence of electrical noise, optical noise and their correlation on frequency and operating current is analyzed to evaluate the effect of aging on device behavior and reliability.

The aim of the carried out investigation of nitride-based blue light-emitting diodes was to clear up noise origins and their relation to the device aging processes.

## 1. Literature Review

Low-frequency noise (LFN) is a powerful tool for the characterization of the quality, reliability and degradation of optoelectronic devices such as light emitting diodes (LEDs), photodiodes and laser diodes [4,5]. In contrast to conventional techniques based on electrical parameters such as DC or AC measurements, LFN provides better sensitivity to subtle device imperfections and aging processes which may not be immediately reflected in the observable performance of the device. The presented literature review critically reviews the results of different studies on low frequency noise measurements as a tool for the reliability and quality assessment of LEDs and photodiodes [5,6].

### 1.1 Noise Types and Origins in Semiconductor Devices

Electrical noise is an inevitable phenomenon in semiconductor devices caused by the random motion and interaction of charge carriers. Noise has traditionally been considered undesirable, but studies have shown that it is a powerful diagnostic tool to assess the internal condition, material quality and reliability of electronic devices [1]. Low frequency noise has attracted much attention, in particular, because of its high sensitivity to microscopic defects and degradation mechanisms that are not readily detectable by conventional electrical measurements [1,2].

In contrast to the so-called direct current (DC) or usual electrical characterization techniques, noise analysis can provide information about the dynamical fluctuations that occur inside a device. These fluctuations [1ns are directly connected with the transport of carriers, defect states, and structural imperfections. Thus, it is important to study the nature and characteristics of different types of noise to understand the behavior of semiconductors and to assess the quality of the device [2,3].

### 1.2 Classification of Noise Mechanisms

Electrical noise in semiconductor devices can be classified into several types according to their physical origin [7]. The most important noise mechanisms include thermal noise, shot noise, generation–recombination noise, random telegraph signal (RTS) noise, and 1/f noise [7,8]. Each of these noise types is related to a specific physical process and provides certain information about the device [7].

### 1.2.1 Thermal Noise

Thermal noise (or Johnson–Nyquist noise) is the noise generated by the random thermal motion of charge carriers in a conductor. It is present in all resistive materials and exhibits a flat (white) spectral density over a wide frequency range. The voltage noise spectral density is given by [9]:

$$S_V = 4kTR; \qquad \ldots\ldots\ldots\ldots\ldots\ldots\ldots\ldots [1]$$

Where, $k$is the Boltzmann constant, $T$is the temperature, and $R$is the resistance. Since thermal noise depends only on temperature and resistance, it is generally independent of defects or material quality. However, it still plays an important role in device characterization. For example, it can be used to calibrate measurement systems, determine temperature in harsh environments, and evaluate the quality of thermal contacts between layers. An increase in thermal noise under bias conditions may indicate poor heat dissipation or delamination in thin-film structures, leading to early device failure [10].

### 1.2.2 Shot Noise

Shot noise is a consequence of the discrete nature of electric charge and occurs when carriers cross a potential barrier, such as in diodes and junction-based devices [11]. The present noise spectral density is written as:

$$S_I = 2qI; \qquad \ldots\ldots\ldots\ldots\ldots\ldots\ldots\ldots [2]$$

Where q is the elementary charge, and I the mean current.

In the ideal devices the shot noise scales linearly with the current. However, deviations from this behavior can indicate the presence of non-idealities such as leakage currents, parasitic resistance or recombination processes [5]. For low current levels deviations can reveal shunt paths and at high electric fields an increase over the expected value can be suggestive of carrier effects of multiplication [5]. These properties make shot noise a useful diagnostic for diode-type devices, and for assessing their quality [10].

### 1.2.3 Generation–Recombination Noise

Generation–recombination (g–r) noise originates from fluctuations in the number of charge carriers due to trapping and detrapping at defect sites within the semiconductor. These fluctuations lead to fluctuations in the conductivity and give rise to a characteristic Lorentzian spectrum [5].

The energy levels and the density of trap states have a strong influence on the g-r noise behavior. If the trap energy level is close to the Fermi level, it participates in the active carrier exchange, which gives considerable noise [5]. On the other hand, traps far from the Fermi level are inactive and do not contribute significantly.

Such noise is particularly useful in studies of processes related to defects in semiconductors. It provides useful information on trap densities, carrier lifetimes and recombination mechanism [5]. In many cases, g–r noise analysis complements other techniques like deep-level transient spectroscopy (DLTS) and provides a simpler, non-destructive alternative [3].

### 1.2.4 Random Telegraph Signal Noise

Random Telegraph Signal (RTS) noise is a discrete switching between two or more current levels. It is caused by the capture and emission of carriers by individual trap centers and is generally found in devices with small numbers of carriers [5].

The RTS noise is very prominent, especially in modern small-scale devices as a single defect can drastically affect the device behavior [5]. The magnitude of the fluctuations can be quite large relative to the average current, making RTS noise a powerful marker of localized defects or poor material quality.

The appearance of RTS noise is also a function of bias conditions and temperature as it is the activity of trap states that is influenced by these factors [5]. It is common to consider devices with RTS noise as less reliable because the underlying defects can accelerate the degradation [10].

### 1.2.5 1/$f$ Noise and Its Physical Origin

Among all the noise mechanisms, 1/f noise (flicker noise) is the most important one for reliability analysis and material characterization. Its spectral density decays as inverse frequency and is usually written as:

$$S(f) = C / f^m ; \qquad \text{……………………………………..} \ (3)$$

where m≈1 and $S(f)$is the power spectral density (PSD) of the noise signal at frequency $f$, $C$ is a proportionality constant, $f$is the frequency, and $m$is the frequency exponent, which is typically close to 1 for $1/f$noise.

Unlike thermal and shot noise, 1/f noise is strongly dependent on the internal structure and quality of the material. This is usually attributed to two main mechanisms [5]. Carrier mobility fluctuations are caused by variations in carrier scattering due to lattice vibrations, impurities, or defects. Carrier number fluctuations, resulting from trapping and detrapping of carriers at defect sites

**1.3 Dependence of 1/$f$ Noise on Material Quality and Structural Defects**

Although there is no single universal explanation, both mechanisms are widely accepted as contributing to 1/f noise, depending on the device and material conditions. One of the most important parameters to quantify the 1/f noise is the noise coefficient α, also known as the Hooge noise parameter, which expresses the contribution of individual carriers to the total noise [5]. This parameter was introduced by Hooge to normalize and compare the relative 1/f noise levels in different materials and devices. The Hooge empirical relation for 1/f Noise is written as:

$$\frac{S_R}{R^2} = \frac{\alpha}{fN}; \qquad \ldots\ldots\ldots\ldots\ldots\ldots\ldots\ldots\ldots\ldots\ldots \text{(4)}$$

where S R is the power spectral density of resistance fluctuations, Ris is the resistance, f is the frequency, N is the total number of free charge carriers, and α H. Experimental studies have shown that this parameter strongly depends on the crystal quality and defect density [5]. Materials with greater impurity levels or structural damage have much higher values of alpha, which implies higher noise levels [5].

One of the most important results from classical studies is the strong relation between 1/f noise and material quality. The magnitude of 1/f noise directly depends on several factors related to the internal structure of semiconductor material [5]. Crystal defects and lattice imperfections, impurity concentrations, roughness of the interface, surface states, scattering mechanisms in the material. These factors cause fluctuations in the carrier transport, which directly contribute to the generation of low frequency noise. Thus, high density of defects in a material corresponds to high noise while high quality of a material with small defects corresponds to low noise behavior.

Experimental results show a large increase of 1/f noise with the introduction of defects e.g. by irradiation or mechanical stress [5, 3]. Materials with fewer defects, however, show lower noise levels and better electrical behaviour [5]. A major advantage of noise analysis is its high sensitivity to small structural imperfections. Classical studies have shown that even small imperfections like voids or local defects can lead to a large increase of the noise, whereas no significant changes can be detected in the resistance [2,11]. This indicates that the noise measurements are more sensitive to the microscopic changes in the material structure than the conventional electrical characterization techniques.

This behavior can be understood by noticing that noise is affected by local fluctuations of current density [5]. Current crowding occurs in defective areas, which enhances fluctuations and increases noise. Therefore, even a small structural defect can significantly affect the noise performance of semiconductor devices.

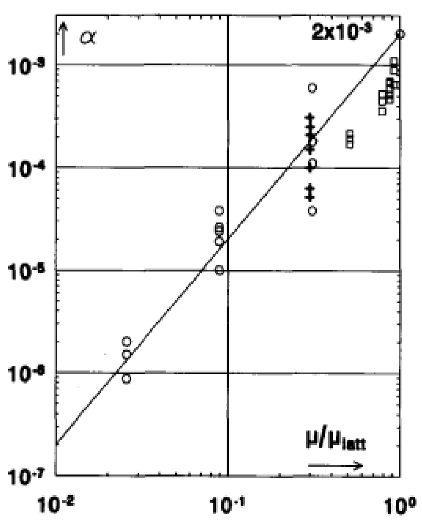


Fig. 1: 1/$f$ noise dependence on material quality [5].

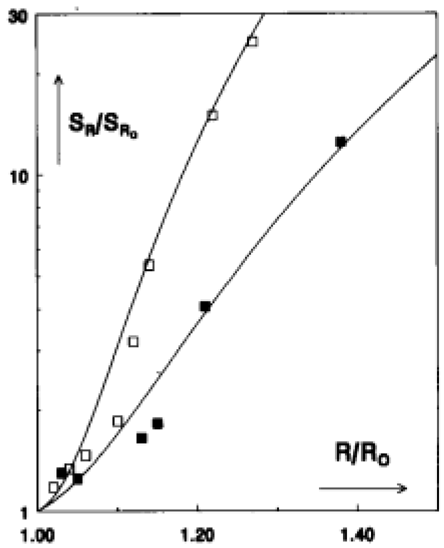


Fig 2: Comparison of resistance and noise increase due to defect formation, demonstrating that higher sensitivity of noise measurements should be merged into one [5].

### 1.4 Effect of Contacts and Current Crowding

Another important origin of noise is related to electrical contacts and current distribution. Non-uniform current flow, also known as current crowding, can significantly enhance noise levels [5]. Poor contacts or interface irregularities create localized regions of high current density, which increase fluctuations and lead to higher $1/f$ noise [5].

This effect is particularly important in modern devices, where small dimensions and high current densities make them more sensitive to contact-related issues. Noise analysis can therefore be used to evaluate contact quality and detect early-stage degradation [11].

### 1.5 Noise Characteristics in LEDs and Photodiodes

Low frequency noise (LFN), including $1/f$ Noise is an important characteristic observed in optoelectronic devices. LFN in these devices is mainly due to material defects and changes in carrier mobility or free-carrier concentration [3,5]. The $1/f$ noise in LEDs occurs due to the interaction between the charge carriers and the defects of the matrix of the semiconductor, thus the $1/f$ noise affects the performance and reliability of the LED [2,6].

Similar processes take place in photodiodes, and here LFN can be due to variations in the photocurrent and to the natural quality of the semiconductor material. The relationship that exists between electrical noise and optical noise in LEDs and photodiodes provides useful data about their degradation with time, and can be used for predictive maintenance and reliability measurement [11].

Minimizing $1/f$ noise requires improving material quality and designing device structures that reduce defects, thus enhancing performance and reliability [5]. Some of the techniques, which include optimization of the growth process and the utilization of high-purity materials, are helpful in reducing the occurrence of defects in the active region of the device [2].

### 1.6 Noise Characteristics, Aging Effects, and Reliability in LEDs and Laser Diodes

The significance of aging experiments as a fundamental methodology is that they enable us to understand how the noise properties of optoelectronic devices evolve with time. The aging of light emitting diodes (LEDs) leads to the slow deterioration of the internal structure of LEDs often more clearly revealed in the noise characteristics than in the usual optical performance.

Palenskis et al. (2010) reported significant differences in the electrical noise behavior in the aging process, on a comparative evaluation of nitride-based green (InGaN) and phosphide-based red (AlInGaP) LEDs [2]. The luminous flux of red LEDs was almost unchanged, but the electrical noise increased due to leakage currents caused by defect propagation. This observation indicates the potential for internal degradation even if the conventional parameters of performance seem stable [2].

In LEDs, aging-induced electrical noise is typically associated with leakage currents and defect generation. Pralgauskaite et al. (2015) showed that electrical noise is a more sensitive indicator of aging compared to optical performance, and a strong correlation between electrical and optical noise was observed in green LEDs [6].

Electrical noise in LEDs due to aging is often connected with leakage currents and generation of defects. Pralgauskaite et al. (2015) demonstrated that electrical noise is a more sensitive indicator of aging than optical performance and a strong correlation between electrical and optical noise was observed in green LEDs [6].

However, the use of low frequency noise (LFN) as a predictor of aging should be considered with caution. Bychikhin et al. [10] showed that the series resistance noise, which is a major contributor to LFN in GaN-based LEDs, is strongly aging-dependent and increases significantly under thermal and electrical stress conditions. Some studies consider the degradation in the active region, however external factors such as the degradation of contact resistance can also be of significant importance in the noise behavior [2,6,10]. This suggests that both internal and external mechanisms have to be included in the evaluation of noise-based aging effects.

During aging, the noise properties of LEDs and photodiodes can change. Aging often leads to an increase in defect density, resulting in higher LFN and deteriorated performance [6,10]. As an example, the electrical noise of an ageing LED can increase due to the development of leakage currents caused by defects that develop in the material [2, 6]. Through measurement of these noise variations, whereby the emergence of degradation is tracked before overt signs of failure are evident, the noise measurement becomes a very valuable instrument in quantifying the reliability and life time of the optoelectronic equipment [11].

Similarly, the noise characteristics of laser diodes, as optoelectronic devices, provide useful information regarding their stability in operation and their long-term reliability. The 1/f noise dominates in laser diodes at lower bias currents and is mainly attributed to fluctuations of carrier mobility and concentration caused by material defects such as dislocation and impurity [5,3].

The correlation between electrical and optical noise in laser diodes was also investigated by Pralgauskaite et al. (2010), who showed that a strong positive correlation indicates stable device operation [2]. On the other hand, a weak or negative correlation shows the existence of defects such as leakage currents or electromigration, which can cause material degradation.

The relationship between electrical and optical noise in laser diodes was also studied by Pralgauskaite et al. (2010), who concluded that a strong positive correlation indicates stable device operation [2]. A weak or negative correlation, on the other hand, indicates the presence of flaws such as leakage currents or electromigration that can lead to material degradation.

The study of low-frequency noise in both LEDs and laser diodes results in a deeper knowledge of degradation mechanisms, defect evolution, and reliability, in general. Electrical noise, optical noise, and their correlation allow for identification of early stage degradation, enhancement of device design, maintenance strategies, and long-term performance.

### 1.7 Noise as a Diagnostic Tool for Defects in Optoelectronic Devices

It was determined by Vandamme (1994) that noise $1/f$ and $1/f^2$ of the noise are especially susceptible to degradation processes, including current crowding, contact degradation, and electromigration, that are hard to trace by conventional techniques [11]. This was also reinforced by Jones (2002), who demonstrated that excess noise is more or less related to device degradation and that LFN is a reliable indicator of early failure [3].

Along with the conventional electrical measurements, Jones (1994) and Hooge (1994) pointed out that noise measurements would help to detect defects that are not obvious to a more standard test, either an imperfection in the material or damage occurring during electromigration [5,3]. Hence, LFN offers a non-destructive, extremely sensitive, and efficient method of predicting the lifetime of optoelectronic equipment and has a diagnostic benefit over other characterization methods [11].

The analyzed papers all indicate that low-frequency noise (LFN) has great potential as the diagnostic tool to detect defects in optoelectronic devices, specifically in light-emitting diodes (LEDs) and laser diodes [11]. Jones (2002) also carried out a study that further supported this conclusion, demonstrating that excess noise is strongly correlated with the degradation of the device, and LFN measurements can be successfully used to detect the early stages of device failures [3].

Besides conventional electrical measurements, Jones (1994) and Hooge (1994) pointed out that $1/f$ provides a sensitive and non-destructive method for evaluating material quality and reliability in optoelectronic devices [5,3]. Therefore, the low-frequency noise levels measurement is a non-destructive, high-sensitivity, and efficient method of determining the reliability of devices and the life span of the optoelectronic components that have invaluable diagnostic benefits as compared to the traditional characterization techniques [11].

Research indicates that LFN can identify an early warning of a device failure, which makes it a very effective diagnostic attribute of determining the life of a device [3,11]. With the aging of optoelectronic devices, LFN measurements can monitor variations in the level of noise, and it is thus a dependable way of keeping track of the changes with time [6]. All in all, LFN is an essential instrument in quality management and control of optoelectronics, which can be beneficial compared to the conventional measurement methods as it can identify problems before they can affect visible performance [11].

### 1.8 Quality and Reliability Issues of Nitride-Based Devices

Nitride-based semiconductor devices, particularly those based on gallium nitride (GaN) and indium gallium nitride (InGaN), have become essential in modern optoelectronics due to their high efficiency, wide bandgap, and thermal stability. But the quality of the materials and the defect density have a strong impact on their performance and long-term reliability One of the major problems for nitride-based devices is the high density of structural defects, such as threading dislocations, point defects and interface-related imperfections. These defects are mainly due to the lattice mismatch during the epitaxial growth and act as trapping centers for carrier transport. This causes variations of carrier mobility and concentration, and hence, increases the low frequency noise levels and degrades the device performance [10].

From the reliability point of view, these defects lead to an increase of leakage currents, nonradiative recombination and gradual degradation of the active region. Studies have proved that noise measurements are more sensitive than conventional DC parameters to detect early degradation mechanisms, and therefore are very suitable for reliability evaluation [3].

### 1.9 Low-Frequency Noise in Nitride-Based LEDs and Laser Diodes

The inherently high defect density of nitride based materials makes low frequency noise an important parameter to characterize device behavior. Experimentally it was found that the magnitude of 1/f noise increases with defect density and electrical stress, which provides useful insight into degradation mechanisms and carrier transport processes [10]. And it has been observed that the noise characteristics change drastically under stress conditions even if the optical output is relatively stable. Therefore, noise analysis can provide access to hidden degradation processes that are not accessible to standard electrical or optical measurements and is a powerful tool for device reliability assessment [10].

### 1.10 Defects and Noise Mechanisms in Nitride-Based Optoelectronic Devices

Defects in nitride-based optoelectronic devices play a critical role in determining their electrical and optical noise characteristics. These defects include threading dislocations, vacancies, impurities, and interface traps, all of which contribute to fluctuations in carrier transport and recombination processes [10].

## 2. Noise Measurement Technique and Investigated LEDs

### 2.1 LEDs Investigated

The experiment was conducted using two blue LEDs, one with a wavelength of 455 nm and the other with a wavelength of 470 nm. The investigated blue LEDs are commercially available InGaN-based devices widely used in illumination and optoelectronic applications. InGaN-based devices are widely used in illumination and optoelectronic applications. The datasheet states that blue LEDs typically have emission wavelengths in the range of 455 nm to 470 nm [12,13]. The selected LEDs with peak wavelengths of 455 nm and 470 nm fall within this range and are suitable for investigating low-frequency noise characteristics.

Both LEDs were operated under forward bias conditions specified by their nominal datasheet parameters. The 455 nm LED has a typical forward voltage in the range of 2.75 V to 3.25 V at the forward current of 350 mA [12], whereas the 470 nm LED has a typical forward voltage in the range of 2.70 V to 3.20 V at the forward current of 350 mA [13]. The safe operating area for all electrical and optical noise measurements was calculated with these datasheet values to maintain stable device operation and avoid thermal or electrical degradation during measurements.

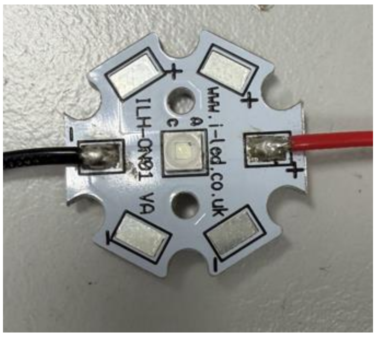


**Fig 2.1:** LED used in the experiment.

The selection of these LEDs was based on their stable optical emission, high luminous efficiency, and suitability for studying electrical and optical noise behavior in semiconductor devices. The two samples have slightly different emission wavelengths, which allow us to compare changes in the material composition and bandgap, and their effects on the noise properties.

## 2.2 Measured Characteristics

The following properties were studied experimentally: I-V characteristics of 455 nm and 470 nm blue LEDs, frequency dependence of the electrical voltage noise spectral density for both LEDs, frequency dependence of the optical noise spectral density for the 455 nm and 470 nm blue LEDs, electrical noise spectral density at different currents for both LEDs at reference frequency 1 kHz, optical noise spectral density at different bias currents at 1 kHz, and average correlation of noise at different operating currents for both LED samples. All measurements were carried out under controlled laboratory conditions. The temperature was kept constant at room temperature ($T$ = 293 K) during the whole experiment. The bias current was swept over a range from 10 nA to 514 mA, depending on the measurement requirements and the devices' safe operating limits.

The frequency range used for noise analysis was 10 Hz to 20 kHz, which is suitable for investigating low frequency noise behavior of optoelectronic devices. For the implementation of a current-dependent analysis, a reference frequency of 1 kHz was selected, providing a stable point for comparing noise performance under different biasing conditions.

## 2.3 Measurement Setup and Equipment

The measurement setup consisted of the following components and instruments. The optical and electrical noise characteristics were investigated with blue LEDs of 455 nm and 470 nm as the main test samples.

To control and stabilize the LED bias current, a resistor network was used. It consisted of high-power resistors (5 W, (680–22) kΩ) in series and parallel combinations. This prevented damage from overcurrent. The LED under test was mounted on a heat sink with thermally conductive white paste to ensure good heat transfer and stable operating conditions. The LED current was controlled by a potentiometer and precisely adjusted from 10 nA to 514 mA. For low current operation, a DC power supply (12 V) was used, while for higher current conditions, two batteries were connected in series. The electrical connections were soldered, ensuring stable, reliable contact. To monitor temperature during operation, a thermoresistor PT100 was used.

For optical measurements, fluctuations of the emitted light from the 455 nm and 470 nm LEDs were detected with a silicon photodiode with a spectral sensitivity range of (400–1100) nm. The photodiode converted the incident light into an electrical current signal, which was then amplified and measured for a precise optical noise analysis.

For electrical characterization, a semiconductor device analyzer, B1500A, was used to obtain I-V characteristics. Due to the limited range of the semiconductor device analyzer at higher currents and voltages, additional measurements were performed using an external circuit setup with a power supply, voltmeter, and ammeter. The two methods were combined to produce the final I–V curve, providing a complete and continuous characterization.

The accelerated aging setup for the studied blue LEDs includes a high-current source that was applied to stress the LED mounted on a PCB and thermally coupled to a heat sink for stable operation. To avoid direct optical interaction during aging, a shielding sheet was placed between the LED and the photodiode. The LED samples were subjected to accelerated aging at 293 K and 350 mA under controlled conditions to simulate long-term device degradation.

The experimental setup for the measurement consisted of two amplifiers, one for the electrical noise signal and one for the optical noise signal from the photodiode. The input signal was connected to the respective amplifier, and the amplified output was first checked with an oscilloscope to assess signal quality and ensure there were no unwanted peaks or disturbances. Once it was confirmed that the signal was stable and suitable for analysis, an additional amplification stage was added to boost the signal level. Finally, the processed signal was connected with a noise analyzer system. The data were recorded by computer-based software for further spectral analysis.

### 2.4. Electrical And Optical Noise Spectra

The electrical and optical voltage noise spectral densities of the 455 nm and 470 nm blue LEDs were studied as a function of frequency and bias current to evaluate the influence of accelerated aging on the device behavior. Noise spectra were measured at different current levels before and after aging in the frequency range from 10 Hz to 20 kHz. The electrical noise measurements were performed directly from the LED electrical signal, and the optical noise measurements were performed under optical detection conditions with a silicon photodiode connected to the noise analyzer. The obtained spectra were plotted as ($S_{u,\mathrm{electrical}}$ vs (*f*) and ($S_{u,\mathrm{optical}}$ vs (*f*), and the noise values at 1 kHz were extracted in order to compare pre-aging and post-aging conditions and to evaluate the dependence of noise characteristics on the applied current. The electrical noise spectral density was calculated using the following relation:

$$S_{u,\mathrm{electrical}} = \frac{S_u - S_{\mathrm{short}}}{S_{\mathrm{ref}} - S_{\mathrm{short}}} \cdot 4k_B \mathrm{T}\, \mathrm{R_{ref}}; \;\ldots\ldots\ldots\ldots\ldots\ldots\; (5)$$

where $S_{u,\text{electrical}}$ is the electrical voltage noise spectral density, $S_u$ is the measured voltage noise spectral density, $S_{\text{short}}$ is the system's own noise when the amplifier is connected to a short, $S_{\text{ref}}$ is the reference resistor's noise spectral density, $k_B$ is the Boltzmann constant, and $T_{\text{ref}}$ is the reference resistor's temperature. This approach allows a direct comparison of noise characteristics and provides insight into aging-induced changes related to defect generation in the devices. The optical voltage noise spectral density was calculated using the following relation:

$$S_{u,\text{optical}} = \frac{S_u - S_{\text{short}}}{S_{\text{ref}} - S_{\text{short}}} \cdot 4k_{\text{B}}T\, R_{\text{ref}}; \ \ldots\ldots\ldots\ldots\ldots\ldots\ldots\ldots (6)$$

where, $S_{u,\text{optical}}$ is the optical voltage noise spectral density, $S_u$ is the measured voltage noise spectral density, $S_{\text{short}}$ is the system's own noise when the amplifier is connected to a short, $S_{\text{ref}}$ is the reference resistor's noise spectral density, $k_B$ is the Boltzmann constant, and $T_{\text{ref}}$ is the reference resistor's temperature.

### 2.5. Cross-Correlation Between Optical and Electrical Noise Signals

The correlation between electrical and optical fluctuations of 455 nm and 470 nm blue LEDs was analyzed as a function of bias current before and after accelerated aging. Correlation values were obtained directly from the noise analyzer software at each current level. The average correlation factor $K$ was determined using the relation:

$$K = \frac{\langle u_{\text{electrical}}(t)\, u_{\text{optical}}(t)\rangle}{\sqrt{\langle u^2_{\text{electrical}}(t)\rangle\, \langle u^2_{\text{optical}}(t)\rangle}}; \ \ldots\ldots\ldots\ldots\ldots (7)$$

where $u_{\text{electrical}}(t)$ and $u_{\text{optical}}(t)$ represent the electrical and optical noise signals, respectively, and $\langle\cdot\rangle$ denotes time averaging.

## 3. Results

### 3.1. Current-Voltage Characteristics of Blue LEDs

The I-V (current voltage) characteristic of blue LEDs of 470 and 455 nm was measured to estimate their performance at different voltages.

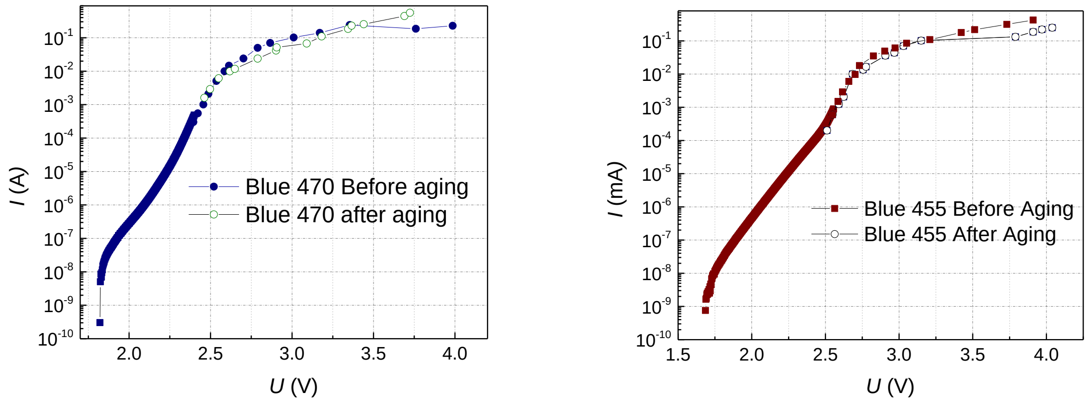


Fig. 3.1. Current–voltage characteristics of blue LEDs 455 and 470 before and after aging

Fig. 3.1(a) and Fig. 3.1(b) show the current–voltage (I–V) characteristics of the investigated blue LEDs of 470 nm and 455 nm at room temperature (293 K) under pre-aging and post-aging conditions. In both devices, an exponential increase in the current with the applied voltage is observed, which is characteristic of the behavior of p-n junction diodes. After aging, at higher voltage levels, small deviations in the curves are observed, indicating small changes in the electrical conduction mechanisms.

The I–V non-ideality factor *n* was estimated from the diode equation:

$$I = I_s \left[ \exp\left(\frac{qV}{nkT}\right) - 1 \right]; \ldots\ldots\ldots\ldots\ldots\ldots\ldots\ldots (7)$$

where q is the elementary charge, k is the Boltzmann's constant, T is the absolute temperature. The computed values are $n$=3.1 for 470 nm LED and $n$=2.9 for 455 nm LED. The values indicate a deviation from the ideal behavior, where $n$=1 corresponds to the diffusion current, $n$=2 corresponds to the recombination current, and values greater than 2 suggest the presence of series resistance effects and defect-related current components [2,6].

As shown in Fig. 3.1(a), the current-voltage characteristics of the 470 nm LED changed little with aging. In the higher voltage region, electrical behavior is mainly influenced by series resistance effects. Fig. 3.1(b) shows that the 455 nm LED maintains comparatively stable characteristics, with only minor variation after aging. The difference in the I–V characteristics reflects variations in material properties and defect density, with the 470 nm LED showing a stronger influence of non-ideal effects.

### 3.2. Light Output Power vs. Current Characteristic

Fig. 3.2 shows the optical output power (P) as a function of current (I) for 455 nm and 470 nm blue LEDs, measured at room temperature (293 K), both before and after aging. In all cases, the optical power increases with increasing current, which is consistent with the behavior of light-emitting diodes, where higher injection current results in increased radiative recombination.

For the 455 nm blue LED, higher optical output power is observed compared to the 470 nm LED at the same current levels, indicating higher optical efficiency. After aging, an approximately 20% decrease in optical power is observed, particularly at higher current levels, indicating degradation of the optical performance. For the 470 nm LED, the optical power increases more gradually with current. After aging, only a minor change in optical output is observed, and the overall optical power remains lower than that of the 455 nm LED over the entire current range.

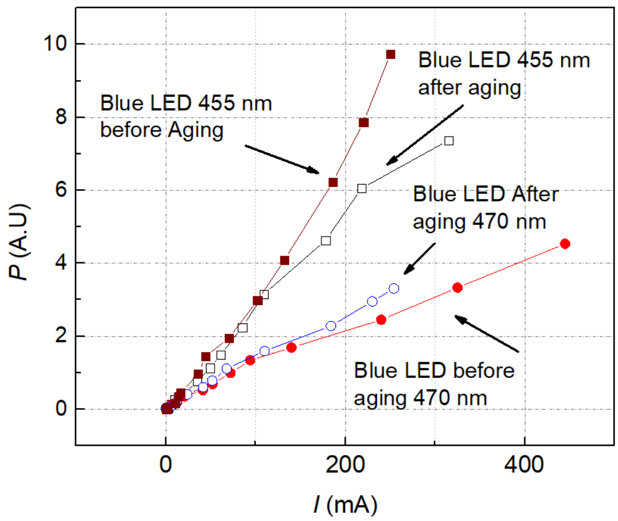


**Fig. 3.2.** Optical light output power of blue LED 455 nm and 470 nm before and after aging.

The observed differences between the two LEDs can be associated with variations in material properties, bandgap energy, and internal quantum efficiency. The results indicate that the 455 nm LED requires lower current to achieve a given optical power compared to the 470 nm LED.

### 3.3. Electrical Noise Spectra

The electrical voltage noise spectral density ($S_{u\ \mathrm{electrical}}$) versus frequency ($f$) of the 455 nm blue LED at different current levels is shown in Fig. 3.3.1 Graph (a) represents the behavior before aging at room temperature (293 K), where the noise spectral density decreases with increasing frequency for all current levels. The electrical voltage noise spectral density $S_{u,\mathrm{electrical}}$ ($f$) of the 455 nm blue LED at different current levels is shown in Fig. 3.3.1. Before and after aging, the spectra exhibit a typical $1/f$ noise behavior, characterized by a gradual decrease in $S_{u,\mathrm{electrical}}$ ($f$) with increasing frequency. This type of noise is commonly associated with carrier trapping and detrapping processes, structural defects, and fluctuations in carrier mobility within the semiconductor material.

Before aging, the noise spectra show dependence on the applied current, indicating that the electrical noise characteristics are influenced by carrier injection conditions. After aging, changes in the noise magnitude and spectral behavior are observed, suggesting modifications in defect states and carrier transport processes caused by device degradation. Graph (b) shows the same measurement after aging.

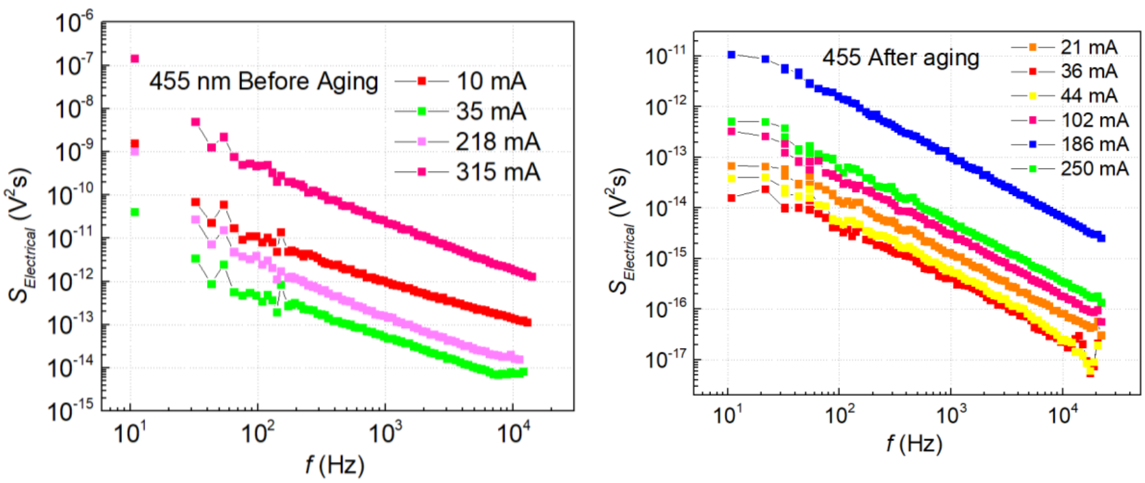


**Fig. 3.3.1** Electrical voltage noise spectral density dependence on frequency at different current levels at room temperature (293 K) of the 455 nm blue LED: (a) before aging and (b) after aging.

 A similar decreasing trend with frequency is observed; however, variations in noise levels across different currents indicate the influence of aging on the device.

The electrical voltage noise spectral density ($S_{u\ electrical}$) as a function of frequency ($f$) for the 470 nm blue LED at different current levels is shown in Fig. 3.3.2 Graph (a) represents the noise spectral density before aging at room temperature (293 K). It can be observed that the noise spectral density decreases with increasing frequency for all applied current levels. Variations in the noise spectral density are observed for different applied current levels, indicating that the electrical noise characteristics depend on the bias current.

Graph (b) shows the corresponding noise spectral density after aging for the same LED. A similar decreasing trend with frequency is observed; however, the distribution of noise levels across different currents is altered. The noise levels after aging remain dependent on current, with noticeable variation between low and high current conditions.

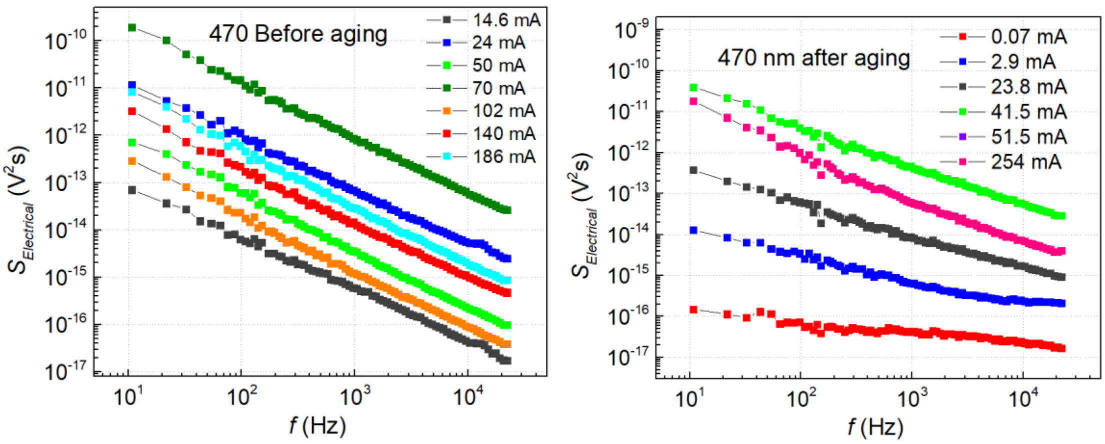


**Fig. 3.3.2** Electrical voltage noise spectral density dependence on frequency at different current levels at room temperature (290 K) of the 470 nm blue LED: (a) before aging and (b) after aging.

The results indicate that electrical noise is strongly influenced by both frequency and current. The electrical voltage noise spectral density depends on the flowing current. Differences between the spectra measured before and after aging indicate that aging influences the electrical noise behavior of the 470 nm blue LED.

### 3.4. Optical Noise Spectra

The optical voltage noise spectral density ($S_{u\ \mathrm{optical}}$) versus frequency ($f$) of the 455 nm blue LED at different current levels is shown in Fig. 3.4.1 Graph (a) represents the behavior before aging at room temperature (293 K). The noise spectral density decreases with increasing frequency for all current levels. The spectra exhibit low-frequency noise behavior with an approximately 1/$f$ type dependence over part of the measured frequency range. Higher current levels correspond to higher optical noise magnitudes due to increased optical output power resulting from higher injection current.

Graph (b) shows the corresponding results after aging. A similar decreasing trend with frequency is observed across all current levels. However, variations in noise magnitude are noticeable compared to the pre-aging condition, indicating that aging affects the optical noise behavior of the device.

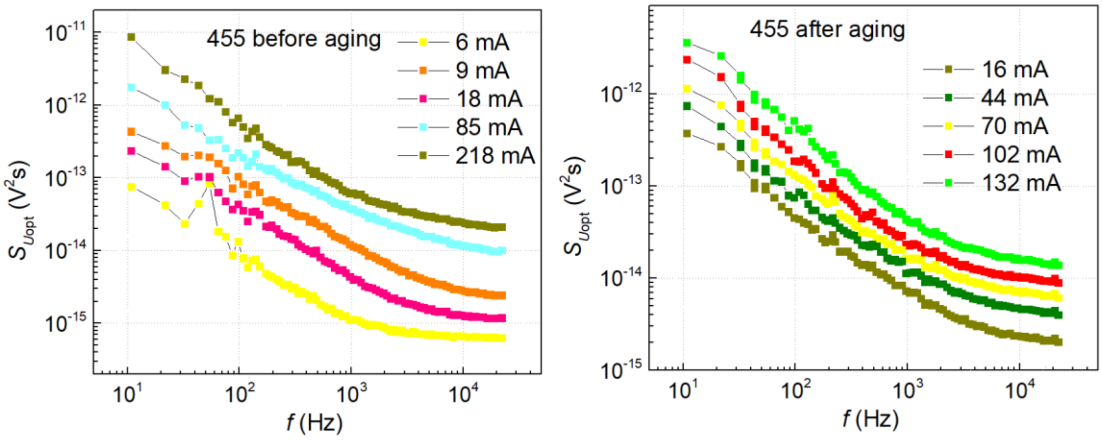


**Fig. 3.4.1** Optical voltage noise spectral density dependence on frequency at different current levels at room temperature (293 K) of the 455 nm blue LED: (a) before aging and (b) after aging.

The optical voltage noise spectral density ($S_{u\ \mathrm{optical}}$) as a function of frequency ($f$) for the 470 nm blue LED at various current levels is presented in Fig. 3.4.2. Graph (a) shows the results before aging at room temperature (293 K). In all cases, the noise spectral density decreases with increasing frequency, following a typical $1/f$ behavior. An increase in current results in a higher noise magnitude, indicating a dependence of optical noise on the bias current.

Graph (b) presents the corresponding measurements after aging. The decreasing trend of noise with frequency is maintained; however, differences in noise levels across the current range become more evident. In particular, low-frequency fluctuations are more pronounced after aging, suggesting modifications in the noise characteristics of the device.

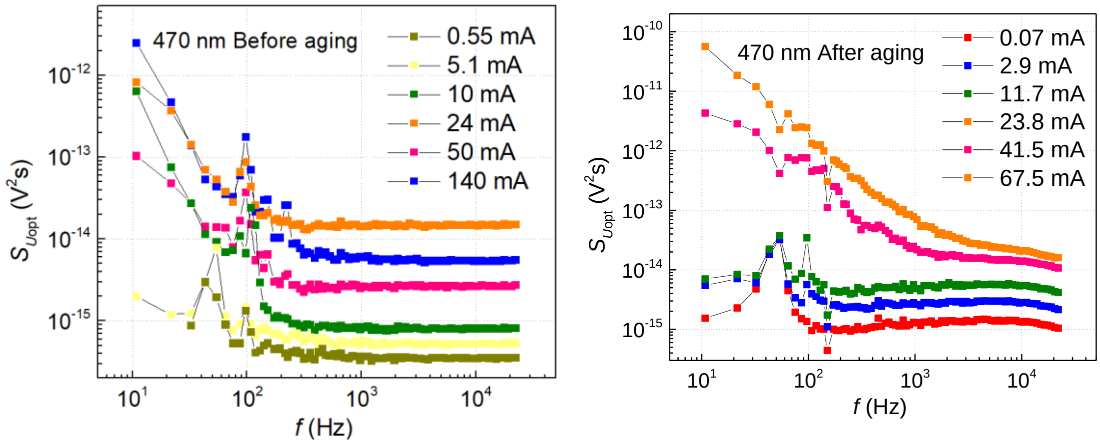


**Fig. 3.4.2** Optical voltage noise spectral density dependence on frequency at different current levels at room temperature (293 K) of the 470 nm blue LED: (a) before aging and (b) after aging.

### 3.5. Noise Characteristics and Cross-Correlation Between Optical and Electrical Fluctuations

Fig. 3.5.1 illustrates the electrical voltage noise spectral density of 455 nm and 470 nm blue LEDs at 1 kHz as a function of current under both pre-aging and post-aging conditions. The data reveal a clear relationship between current and noise level for both LED samples. For the 455 nm LED, the electrical noise level is significantly larger at lower currents compared to the 470 nm LED. The noise decreases with increasing current at lower values, reaches a minimum, and then slightly increases at higher currents. After aging, the electrical noise spectral density of the 455 nm LED decreases by approximately 1–2 orders of magnitude over most of the current range.

For the 470 nm LED, the electrical noise spectral density is considerably lower at low currents and increases with increasing current above approximately 10 mA, approaching the noise level of the 455 nm LED at higher currents. After aging, almost no significant change in the electrical noise level is observed for the 470 nm LED.

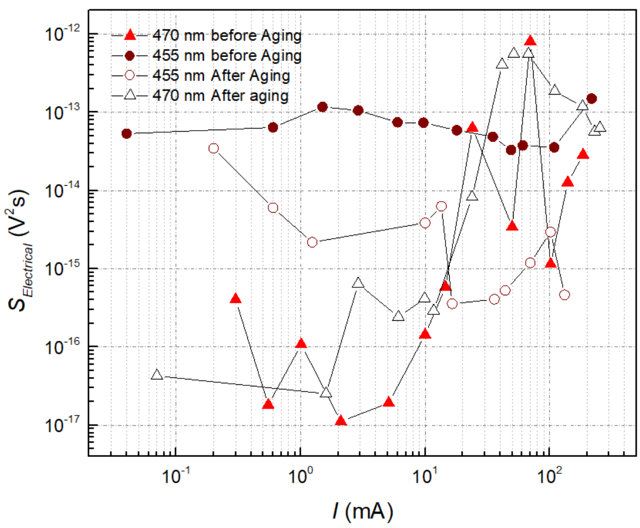


**Fig. 3.5.1** Electrical noise spectral density at various currents of blue LED 455 nm and 470 nm before and after aging at 1 kHz.

Fig. 3.5.2 presents the optical voltage noise spectral density of 455 nm and 470 nm blue LEDs as a function of current at a frequency of 1 kHz under both pre-aging and post-aging conditions. The graph shows an overall increase in optical noise with increasing current for both LEDs. For the 455 nm LED, the optical noise is larger over most of the current range, which may be related to its larger optical output power. The optical noise remains relatively stable after aging with only minor variations observed.

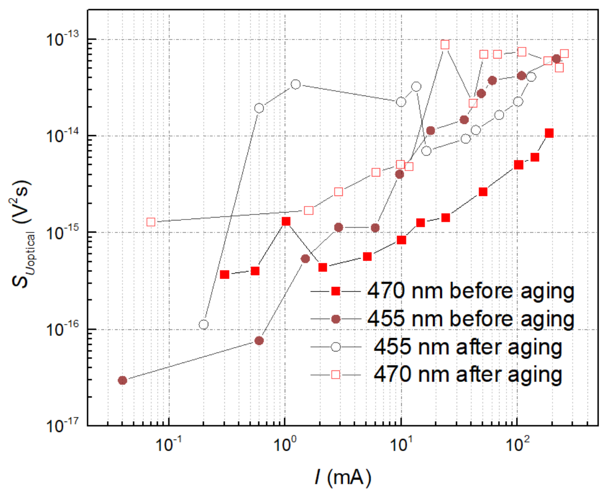


**Fig. 3.5.2** Optical spectral density at various currents of blue LED 455 nm and 470 nm before and after aging at 1 kHz.

For the 470 nm LED, the optical noise increases more noticeably with increasing current and becomes slightly larger after aging. The increase in optical noise after aging may be associated with the slight increase in optical output power observed for the 470 nm LED

Fig. 3.5.3 shows the relationship between the average correlation factor (K) of electrical and optical fluctuations for 455 nm and 470 nm blue LEDs at different current levels under both pre-aging and post-aging conditions. For the 455 nm LED, the correlation factor before aging is large and positive over a wide current range, indicating that the electrical current efficiently flows through the active region and participates in radiative recombination processes. After aging, the correlation factor shifts toward negative values, suggesting the appearance of leakage current channels and degradation-related defects, which may contribute to the reduction in optical output power after aging.

For the 470 nm LED, the correlation factor before aging remains relatively low and slightly positive at higher currents. After aging, the correlation becomes strongly negative over a significant current range, indicating the existence of leakage currents and defect-related transport processes. However, only small changes in electrical noise and optical power are observed after aging, suggesting that these leakage mechanisms do not strongly affect radiative recombination in the active region.

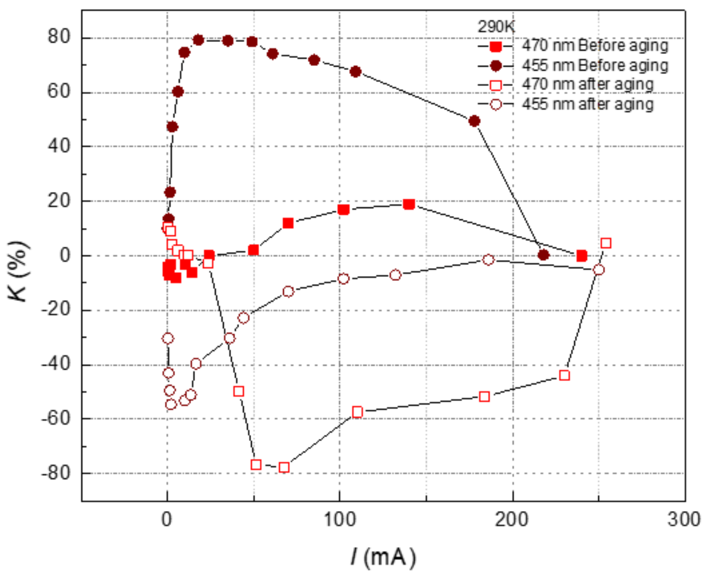


**Fig. 3.5.3** Average correlation factor (K) between electrical and optical fluctuations of blue LED 455 nm and 470 nm before and after aging.

The results indicate that aging affects electrical noise, optical noise, and correlation characteristics differently for the two investigated LEDs. The 455 nm LED exhibits higher electrical and optical noise levels together with a strong positive correlation before aging, while the 470 nm LED shows lower electrical noise and weaker correlation characteristics. After aging, the reduction in correlation and changes in noise behavior indicate the influence of degradation mechanisms and defect generation on carrier transport and optical emission processes in both LED samples.

### 3.6. Discussion

The results obtained show that the electrical, optical, and correlation properties of the investigated blue LEDs of 455 nm and 470 nm differ significantly before and after aging. The light output power of the 455 nm LED is much larger in the investigated current range than that of the 470 nm LED. However, the optical output power of the 455 nm LED is decreased significantly after aging. Meanwhile, the optical output power of the 470 nm LED is slightly increased after aging. These results suggest that the aging process affects the radiative efficiency of the 455 nm LED more than that of the 470 nm LED.

Before aging, the spectral density of the electrical voltage noise of the 455 nm LED is much larger than that of the 470 nm LED. After aging, the electrical noise intensity of the 455 nm LED drops by about 1–2 orders of magnitude over most of the current range. On the contrary, the electrical noise characteristic of the 470 nm LED is relatively stable and almost no significant change is observed after aging. The reduced electrical noise intensity for the 455 nm LED may be explained by the fact that although more defects are generated during the aging process, their contributions are cancelling each other leading to a reduced electrical noise intensity.

The optical voltage noise spectral density of the 455 nm LED is also larger than that of the 470 nm LED, and this could be related to its higher optical output power. The optical noise properties of the aged 455 nm LED do not change significantly, and only small variations are observed. The optical noise slightly increases for the 470 nm LED after aging, which may be related to the observed increase in optical output power after aging. The behavior observed shows that radiative recombination processes and the emitted optical power have a strong influence on the optical noise.

The correlation factor of electric and optical fluctuations provides important information on the carrier transport and recombination mechanisms in the studied LEDs. Before aging, the correlation factor for the 455 nm LED is strongly positive in a wide current region. The high optical output power further indicates that the electrical current efficiently flows through the active region and is part of the radiative recombination processes. The correlation factor turns negative after aging, which implies the appearance of leakage current channels and degradation-related defects. These leakage currents may contribute to the observed decrease in optical output power after aging.

For the 470 nm LED, the correlation factor after aging is strongly negative over a large range of currents, indicating the presence of leakage currents and defect-related transport processes. However, only small changes are observed in the intensity of the electrical noise and in the optical output power after aging. This suggests that the leakage current paths do not play a significant role in the radiative recombination processes in the active region of the 470 nm LED.

## Conclusions

1. The low-frequency electrical and optical noise characteristics of 455 nm and 470 nm blue LEDs were investigated before and after accelerated aging. The results showed that both LEDs exhibit the typical 1/*f* noise behavior, and the noise intensity strongly depends on the operating current. The optical output power and the electrical and optical noise spectral densities of the 455 nm blue LED were higher than those of the 470 nm LED.

2. The optical output power decreased, and the optical and electrical noise intensity increased after aging of the 455 nm LED, while the 470 nm LED exhibited only minor changes in noise and optical power characteristics.

3. The correlation analysis between electrical and optical fluctuations showed a strong positive correlation for the 455 nm LED before aging, which indicates efficient radiative recombination in the active region. However, it changes to negative values after aging, indicating the emergence of leakage current channels that degrade LED operating characteristics.

**References**

[1] L. K. J. Vandamme, "Noise as a diagnostic tool for quality and reliability of electronic devices," IEEE Transactions on Electron Devices, vol. 41, no. 11, pp. 2176-2187, 1994, doi: 10.1109/16.333839.

[2] V. Palenskis, J. Matukas, and S. Pralgauskaitė, "Light-emitting diode quality investigation via low-frequency noise characteristics," Solid-State Electronics, vol. 54, no. 8, pp. 781-786, 2010/08/01/ 2010, doi: https://doi.org/10.1016/j.sse.2010.04.003.

[3] B. K. Jones, "Electrical noise as a reliability indicator in electronic devices and components," IEE Proceedings - Circuits, Devices and Systems, vol. 149, no. 1, pp. 13-22, 2002/02/07 2002, doi: https://doi.org/10.1049/ip-cds:20020331.

[4] U. Doru and K. J. Brian, "Low-frequency noise used as a lifetime test of LEDs," Semiconductor Science and Technology, vol. 11, no. 8, p. 1133, 1996/08/01 1996, doi: 10.1088/0268-1242/11/8/002.

[5] F. N. Hooge, "1/f noise sources," IEEE Transactions on Electron Devices, vol. 41, no. 11, pp. 1926-1935, 1994, doi: 10.1109/16.333808.

[6] S. Pralgauskaitė et al., "Reliability investigation of light-emitting diodes via low frequency noise characteristics," Microelectronics Reliability, vol. 55, no. 1, pp. 52-61, 2015/01/01/ 2015, doi: https://doi.org/10.1016/j.microrel.2014.09.027.

[7] B. K. Jones, "Low-frequency noise spectroscopy," IEEE Transactions on Electron Devices, vol. 41, no. 11, pp. 2188-2197, 1994, doi: 10.1109/16.333840.

[8] X. Y. Chen, A. Pedersen, O. G. Hellesø, and A. D. v. Rheenen, "Electrical noise of laser diodes measured over a wide range of bias currents," Microelectronics Reliability, vol. 40, no. 11, pp. 1925-1928, 2000/11/01/ 2000, doi: https://doi.org/10.1016/S0026-2714(00)00053-6.

[9] S. Pralgauskaite, J. Matukas, and V. Palenskis, "Low Frequency Noise Characteristics of Multimode and Singlemode Laser Diodes," in Semiconductor Laser Diode - Technology and Applications, D. S. Patil Ed. London: IntechOpen, 2012.

[10] S. Bychikhin, D. Pogany, L. K. J. Vandamme, G. Meneghesso, and E. Zanoni, "Low-frequency noise sources in as-prepared and aged GaN-based light-emitting diodes," Journal of Applied Physics, vol. 97, no. 12, p. 123714, 2005, doi: 10.1063/1.1942628.

[11] J. Glemža et al., "Quality evaluation of NIR laser diodes for medical application using low-frequency noise characterization," Infrared Physics & Technology, vol. 147, p. 105794, 2025/06/01/ 2025, doi: https://doi.org/10.1016/j.infrared.2025.105794.

[12] Lemona Electronics, "LED Module, Deep Blue, 455 nm, 1 W," accessed May 12, 2026.

[13] Lemona Electronics, "LED, Blue, 1CD, 470 nm," accessed May 12, 2026.

Faculty of Physics

Institute of Applied Electrodynamics and Telecommunications

Gul Jan

Noise Diagnostics of Optoelectronic Devices

Supervisor: Dr. Sandra Pralgauskaitė

**Summary**

This study investigates the low-frequency electrical and optical noise characteristics of InGaN-based blue light-emitting diodes (LEDs) with peak wavelengths of 455 nm and 470 nm before and after accelerated aging. The aim of this investigation was to clear up noise origins and their relation to the device aging processes. It focuses on understanding how aging affects carrier transport, defect generation, optical emission, and reliability of optoelectronic devices through noise diagnostics.

A literature review was conducted on different noise mechanisms in semiconductor devices, including thermal noise, shot noise, generation–recombination noise, random telegraph signal noise, and $1/f$ noise. Particular attention was given to the role of low-frequency noise as a sensitive, non-destructive diagnostic tool for detecting structural defects, degradation processes, leakage currents, and reliability issues in LEDs and other optoelectronic devices.

Experimental investigations were carried out using 455 nm and 470 nm blue LEDs under controlled laboratory conditions. Electrical current–voltage characteristics, optical output power, electrical voltage noise spectral density, optical noise spectral density, and cross-correlation between electrical and optical fluctuations were measured before and after 30 h of accelerated aging. Noise spectra were analyzed in the frequency range from 10 Hz to 20 kHz at different operating currents.

The results demonstrated typical $1/f$ noise behavior in both LEDs, with the spectral density decreasing with increasing frequency. The 455 nm LED exhibited higher optical output power and significantly larger electrical and optical noise levels compared to the 470 nm LED. After aging, the optical output power of the 455 nm LED decreased, while optical and electrical noise intensity increased. The 470 nm LED showed only minor changes in electrical and optical characteristics.

Correlation analysis between electrical and optical fluctuations revealed a strong positive correlation for the 455 nm LED before aging, indicating efficient radiative recombination within the active region. After aging, the correlation became negative for both LEDs, suggesting the formation of current leakage paths and degradation-related defects that affect carrier transport.

Vilniaus universitetas Fizikos fakultetas

Taikomosios Elektrodinamikos ir Telekomunikacijų institutas

Gul Jan

Optoelektroninių įtaisų triukšmo diagnostika

Vadovė : dr. Sandra Pralgauskaitė

**Santrauka**

Šiame darbe tiriamos InGaN pagrindu pagamintų mėlynos šviesos diodų (ŠD), kurių spinduliuotės bangos ilgiai yra 455 nm ir 470 nm, žemo dažnio elektrinio ir optinio triukšmo charakteristikos prieš ir po 30 val. paspartinto sendinimo. Tyrimo tikslas – ištirti triukšmo šaltinius šiuose dioduose ir išanalizuoti, kaip sendinimas veikia krūvininkų pernašą, defektų susidarymą, optinę emisiją ir optoelektroninių įtaisų patikimumą.

Literatūros apžvalgoje aptariami puslaidininkiniuose prietaisuose pasireiškiantys triukšmo mechanizmai, įskaitant šiluminį triukšmą, šratinį triukšmą, generacijos–rekombinacijos triukšmą, impulsinį triukšmą ir $1/f$ triukšmą. Ypatingas dėmesys skirtas $1/f$ triukšmui kaip jautriam ir neardomajam diagnostikos metodui, skirtam aptikti struktūrinius defektus, degradacijos procesus, nuotėkio sroves ir ŠD bei kitų optoelektronikos prietaisų patikimumo problemas.

Eksperimentiniai optinių ir elektrinių fliuktuacijų tyrimai buvo atlikti naudojant 455 nm ir 470 nm ŠD. Taip pat buvo matuojamos voltamperinės charakteristikos, spinduliuotės galia. Visi matavimai atlikti prieš ir po 30 val. paspartinto sendinimo. Triukšmo spektrai buvo analizuojami 10 Hz–20 kHz dažnio srityje, tekant skirtingo stiprio srovei.

Gauti rezultatai parodė būdingas $1/f$ tipo elektrines fliuktuacijas abiem tirtiem ŠD. 455 nm ŠD pasižymėjo didesne spinduliuotės galia bei žymiai didesniu elektrinio ir optinio triukšmo intensyvumu lyginant su 470 nm ŠD. Po sendinimo 455 nm ŠD spinduliuotės galia sumažėjo, o elektrinio triukšmo intensyvumas išaugo. 470 nm ŠD elektrinės ir optinės charakteristikos po sendinimo pakito nežymiai. Elektrinių ir optinių fliuktuacijų koreliacijos analizė parodė stiprią teigiamą koreliaciją 455 nm LED prieš sendinimą, kas rodo efektyvią spinduliuojamąją

rekombinaciją aktyviojoje srityje. Po sendinimo abiejų ŠD koreliacija tapo neigiama, o tai rodo nuotėkio srovės kanalų susidarymą ir defektus skaičiaus augimą, kurie turi įtakos krūvininkų pernašos procesams.